Since January 2020 Elsevier has created a COVID-19 resource centre with free information in English and Mandarin on the novel coronavirus COVID-19. The COVID-19 resource centre is hosted on Elsevier Connect, the company's public news and information website.

International Journal of Hygiene and Environmental Health 238 (2021) 113833

Contents lists available at ScienceDirect

International Journal of Hygiene and Environmental Health

journal homepage: www.elsevier.com/locate/ijheh

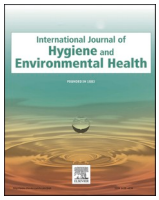

Distinct weather conditions and human mobility impacts on the SARS-CoV-2 outbreak in Colombia: Application of an artificial neural network approach

Santiago Gómez-Herrera [a], Erik Sartori Jeunon Gontijo [a], Sandra M. Enríquez-Delgado [b], André H. Rosa [a,*]

[a] São Paulo State University (UNESP), Institute of Science and Technology, Av. Três de Marco, 511, Alto da Boa Vista, CEP: 18087-180, Sorocaba, SP, Brazil
[b] School of Science, Department of Earth Sciences, EAFIT University, Medellin, Colombia

ARTICLE INFO

Keywords:
COVID-19
Artificial neural network
Biome
Temperature
Humidity
Human mobility

ABSTRACT

The coronavirus disease 2019 (COVID-19) is still spreading fast in several tropical countries after more than one year of pandemic. In this scenario, the effects of weather conditions that can influence the spread of the virus are not clearly understood. This study aimed to analyse the influence of meteorological (temperature, wind speed, humidity and specific enthalpy) and human mobility variables in six cities (Barranquilla, Bogota, Cali, Cartagena, Leticia and Medellin) from different biomes in Colombia on the coronavirus dissemination from March 25, 2020, to January 15, 2021. Rank correlation tests and a neural network named self-organising map (SOM) were used to investigate similarities in the dynamics of the disease in the cities and check possible relationships among the variables. Two periods were analysed (quarantine and post-quarantine) for all cities together and individually. The data were classified in seven groups based on city, date and biome using SOM. The virus transmission was most affected by mobility variables, especially in the post-quarantine. The meteorological variables presented different behaviours on the virus transmission in different biogeographical regions. The wind speed was one of the factors connected with the highest contamination rate recorded in Leticia. The highest new daily cases were recorded in Bogota where cold/dry conditions (average temperature <14 °C and absolute humidity >9 g/m^3) favoured the contagions. In contrast, Barranquilla, Cartagena and Leticia presented an opposite trend, especially with the absolute humidity >22 g/m^3. The results support the implementation of better local control measures based on the particularities of tropical regions.

1. Introduction

The respiratory illness named Coronavirus Disease 2019 (COVID-19) induced by the Severe Acute Respiratory Syndrome Coronavirus 2 (SARS-CoV-2) has rapidly increased its presence across the world since its first occurrence in Wuhan, China, in December of 2019 (Zhou et al., 2020). Based on the magnitude of the emergency, the World Health Organisation (WHO) declared the outbreak a Public Health Emergency of International Concern (PHEIC) in January 2020 and officially a pandemic on March 11th (WHO 2020a, 2020b). This new virus is highly contagious, and the transmission ways include direct contact by secretions of an infected person and indirect contamination via contact with contaminated surfaces (Dhand and Li, 2020; Guarner, 2020; Mouchtouri et al., 2020). The dispersion of this virus depends on social factors (affected by human mobility) and extra-human factors such as environmental conditions that have effects on its inactivation and persistence (Aboubakr et al., 2020; Kubota et al., 2020).

Recent epidemiological studies have shown evidence of significant correlations between the weather conditions and the SARS-CoV-2 cases (Briz-Redón and Serrano-Aroca, 2020a; Fernández-Ahúja and Martínez, 2021; Islam et al., 2021; Kulkarni et al., 2021; Nottmeyer and Sera, 2021; Pan et al., 2021; Rosario et al., 2020; Sanchez-Lorenzo et al., 2021). Temperature, for instance, has apparently two main effects: inhibiting the virus replication under warm conditions or favouring its stability under cold or temperate conditions (Araújo and Naimi, 2020; Bukhari and Jameel, 2020; Notari, 2021; Wu et al., 2020). Other authors highlighted the relevant role of variables such as wind speed and humidity (Coşkun et al., 2021; Diao et al., 2021; Farkas et al., 2021; Wei

* Corresponding author. São Paulo State University (UNESP), Institute of Science and Technology, Sorocaba, SP, Brazil.
E-mail address: andre.rosa@unesp.br (A.H. Rosa).

https://doi.org/10.1016/j.ijheh.2021.113833
Received 27 January 2021; Received in revised form 12 August 2021; Accepted 23 August 2021
Available online 25 August 2021

et al., 2020). Results indicated that the severity of the disease in terms of infections presented marked differences between temperate and tropical countries (Battineni et al., 2020; Tushabe, 2020). This makes the stability of SARS-CoV-2 under different meteorological conditions an important area of study, particularly in tropical countries such as Brazil, Bangladesh, Singapore, Philippines or Indonesia where several outbreaks have been recorded (Auler et al., 2020; He et al., 2021; Hridoy et al., 2021; Pani et al., 2020; Seposo et al., 2021; Tosepu et al., 2020).

The current scenario of the pandemic and the presence of large amounts of data turns essential the use of good tools to cluster and visualise relationships among variables involved in the virus transmission to support control strategies (Yahya et al., 2021). Artificial neural network (ANN) techniques are examples of tools that can be used to perform exploratory analysis of these data and model the spread of the disease to predict future outbreaks (Car et al., 2020; Mollalo et al., 2020; Niazkar and Niazkar, 2020). They are mathematic models and algorithms used to mimic some characteristics of the human brain such as the capacity of learning by examples (Terfloth and Gasteiger, 2001). ANN is formed by basic units named neurons that collect input data, converting them by using a function in output data (Terfloth and Gasteiger, 2001).

Self-organising map (SOM, also known as Kohonen neural network) is an example of ANN that is based on unsupervised learning (Kohonen, 2001; Vesanto, 1999). This technique projects high-dimensional data into a lower-dimensional space with the purpose of grouping samples with similar characteristics and finding possible patterns (Brereton, 2012; Doan et al., 2020). It has outstanding visualisation capabilities, it is ease to implement and robust to missing data (Asan and Ercan, 2012; Vesanto, 1999). In the context of the COVID-19 pandemic, SOM has been used to find similarities in the transmission dynamics among cities, regions or countries worldwide (Galvan et al., 2021; Hartono, 2020; Melin et al., 2020). Other authors focused on evaluating the influence of demographic, socio-economic, and health conditions in the virus spread (Galvan et al., 2020; Khan et al., 2021). Leichtweis et al. (2021) considered the relationship between the virus dissemination rate and some meteorological variables such as environmental temperature, relative humidity and solar radiations with SOM. The study was limited to clustering countries that displayed similar predictor variables.

Colombia is an equatorial country dominated by tropical conditions with climatic variations connected to elevation differences across its territory (Raines et al., 2020). This makes it an ideal place to study the spread of SARS- CoV-2, since the behaviour of the virus under warm climates is still debatable and the country is one of the worst affected countries worldwide (He et al., 2021; Prata et al., 2021; Islam et al., 2020). From July 2020 to January 2021, Colombia was positioned within the 11 countries with the most confirmed cases in the world according to Johns Hopkins University; in September, the country reached the 5th position (Johns Hopkins, 2021). This knowledge would help to implement local health policies and predict when to expect the worst outbreaks in tropical areas where several poorer countries are located (Islam et al., 2020). Furthermore, information about the changes in the meteorological variables in Colombia and the direct relation with the virus spread is still limited, and this investigation intends to fill this gap (De la Hoz-Restrepo et al., 2020)

This paper aims to assess if the weather conditions of different geographical regions in Colombia affect the dissemination of SARS-CoV-2. Mobility variables were included because human contact has an important role in the virus transmission (Marcu, 2021; Shao et al., 2021). Since the results from this type of study are difficult to interpret because of their complexity (due to large amounts of data and variables) and spatial-temporal variability (Khan et al., 2021), we selected the SOM technique because of its visualisation and clustering capabilities. This investigation has the potential to contribute to the development of site-specific public health policies for controlling COVID-19 in Colombia and other tropical countries, where the pandemic is still out of control. We intend to demonstrate the applicability of SOM in this type of study for exploratory analysis that was not performed in Colombia so far.

2. Methodology

2.1. Study area

Colombia is a transcontinental country in Latin America with a population of fewer than 50 million inhabitants. It is formed by 33 administrative regions distributed in a total area of 2.07 million km^2 (Departamento Administrativo Nacional de Estadística, 2018). Since the beginning of the outbreak, the development of the pandemic has been concentrated in the main cities that acted as sources of the disease to other regions of the country (De la Hoz-Restrepo et al., 2020).

Six cities located in five different biomes (humid montane forest, pre-mountain rainforest, subtropical dry forest, tropical dry forest and tropical rainforest) in Colombia were selected to analyse the dissemination of COVID-19: Bogota (BOG), Medellin (MED), Cali (CAL), Barranquilla (BAR), Cartagena (CAR), and Leticia (LET). The main demographic and geographical information of the cities are presented in Table S1 (Appendix A). The localisation of the cities with their respective biomes is shown in Fig. 1. The data was obtained from the Institute of Hydrology, Meteorology and Environmental Studies of Colombia (IDEAM) (http://www.ideam.gov.co/, accessed in April 2021). The classification of the biomes was based on the Holdridge's scheme (Holdridge and Grenke, 1971) and the map was created using ArcGis pro software (v.2.2.4 ESRI, USA).

2.2. Data collection

The first case of coronavirus in Colombia was confirmed on March 6th' 2020 in its capital Bogota. As a result of a fast raise in number of the new cases and the spread of the virus in most of the departments, the

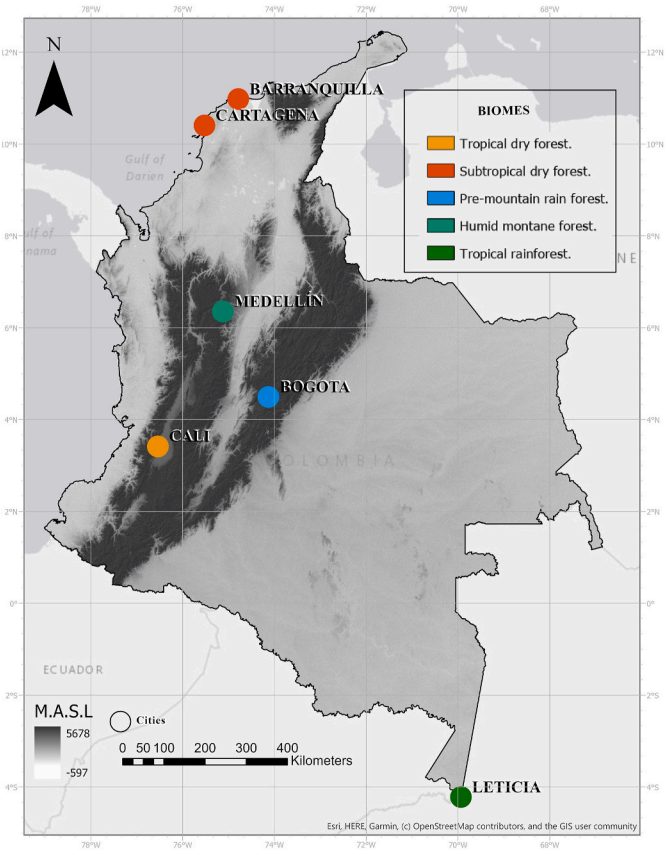

Fig. 1. Map showing the localisation and biome of each studied city.

government decreed a total quarantine with the intent to contain the growing emergence on March 25th (Ramírez et al., 2020). Nevertheless, due to the imminent economic crisis, the state was forced to ease the restrictions in May for some commercial sectors and the end of the mandatory isolation since September 1st, but continuing with the biosafety protocols (Arellana et al., 2020). In January 2021, some restrictions were promulgated aiming to control a new wave of the virus after December festivities.

Data of COVID-19 cases were downloaded from the *Instituto Nacional de Salud* (https://www.ins.gov.co/Noticias/Paginas/Coronavirus.aspx, accessed in April 2021). The epidemiological variables selected in this study for the period from March 25th, 2020, to January 15th, 2021, were new daily cases (NDC) and contamination rate (CR). CR was calculated dividing the number of new daily reported cases by the total population of the city, and then multiplying the result by 100 thousand inhabitants.

The weather data were obtained from the online database archives of the Weather Underground (http://wunderground.com/, accessed in April 2021). This website has as information sources typical weather stations from countries around the world. The meteorological variables evaluated were daily average temperature (T_{avg}), minimum temperature (T_{min}), maximum temperature (T_{max}), relative humidity (RH), absolute humidity (AH), specific enthalpy (h) and wind speed (WS). AH was calculated as per the Clausius Clapeyron equation (1) presented below (Bukhari and Jameel, 2020):

$$AH = \frac{6.112 \times e^{\frac{17.67 \times T_{avg}}{T_{avg}+243.5}} \times RH \times 2.1674}{273.15 + T_{avg}} \quad (1)$$

where AH is the absolute humidity in g/m^3 and T_{avg} is the average temperature in °C.

Average temperature and relative humidity were used to calculate specific enthalpy (h) based on the following psychrometric parameters: saturated vapour pressure (P_{WS}), vapour pressure (P_W), total ambient pressure (P_{tot}) and mixing ratio (X). Specific enthalpy represents the total heat of a mass air (latent heat energy of the water vapour + specific heat of the dry air) and consequently the amount of energy required to change the psychrometric conditions of the air (de Castro Júnior and da Silva, 2021; Spena et al., 2020a, 2020b).The empirical equations of these parameters are presented below:

a) Saturated vapour pressure (Alduchov and Eskridge, 1996):

$$P_{WS} = 6.116441 \times 10^{\frac{7.591386 \times T}{T+240.7263}} \quad (2)$$

where P_{WS} is the saturated vapour pressure in hPa and T is the average temperature in °C.

b) Vapour pressure (Lawrence, 2005):

$$P_W = P_{WS} \times \frac{RH}{100} \quad (3)$$

where P_W is the vapour pressure in hPa and RH is the relative humidity (%).

c) Total ambient pressure (Berberan-Santos et al., 1997):

$$P_{tot} = 1013.25 \times e^{-0.000118 \times E} \quad (4)$$

where P_{tot} is the total ambient pressure and E is the elevation above sea level of each city (BAR: 20 m.a.s.l; BOG: 2630 m.a.s.l; CAL: 1018 m.a.s.l; CAR: 14 m.a.s.l; LET: 96 m.a.s.l; MED: 1495 m.a.s.l).

d) Mixing ratio (Marquet and Geleyn, 2015):

$$X = \frac{621.9907 \times P_W}{P_{tot} - P_W} \quad (5)$$

where X is the mixing ratio in g/kg.

e) Specific enthalpy (Marquet and Geleyn, 2015):

$$h = T \times (1.01 + 0.00189\,X) + 2.5\,(X) \quad (6)$$

where h is specific enthalpy in kJ/kg.

The mobility data was acquired from the Community Mobility Reports provided by Google (https://www.google.com/covid19/mobility/, accessed in April 2021). It was used to assess the influence of human mobility on the spread of the virus (Bochenek et al., 2021). The indices show changes (%) in the number of visitors across different category of places collected by Google applications: retail and recreation (RR), grocery and pharmacy (GP), parks (PK), transport or transit stations (TS), workplaces (WP) and residential (RS). The results were calculated by comparing the mobility values from a given day during the pandemic with a pre-pandemic baseline value of mobility (January 3rd - February 6th, 2020) (Sulyok and Walker, 2021). For the city of LET, only GP and PK variables were available. Furthermore, two weeks of September were not available.

The meteorological and mobility data used for each city in the analysis corresponded to the average of 7–14 days before the reported day. Previous studies have pointed out the relevance of considering the lag effect based on the latency period of COVID-19 from the infected day to the confirmed day (Chen et al., 2020; Dhouib et al., 2021; N. Islam et al., 2020; Xie and Zhu, 2020).

2.3. Statistical analysis

As a result of a non-normal distribution (asymmetry and kurtosis out of range), the Spearman rank correlation (r_s) was selected to evaluate relevant association coefficients (>0.4) among the epidemiological, meteorological and mobility variables in two different periods: quarantine (March/2020–August/2020) and post-quarantine (September/2020–January/2021). The data were standardised by the z-scores method to perform the statistical tests. The software PAST 2.7 was used for all calculations (Hammer et al., 2001).

2.4. Self-organising maps

SOM technique was used to identity relationships between the epidemiological variables (NDC and CR) and the meteorological (AH, h, RH, T_{max}, T_{avg}, T_{min}, WS) and mobility variables (GP, PK, RR, RS, TS and WP) in the six selected cities from Colombia. Similarities in the spreading of the infections among the cities were also evaluated.

The technique consists of neurons arranged in a two-dimensional grid. Each input sample is represented by a vector whose elements correspond to the variables from data collected in each day (epidemiological, meteorological and mobility variables; dimension was 15). The neurons in the output maps have hexagonal lattice and the same dimension of the input vectors. The number of neurons in these maps are defined by the user. The input and output layers in the technique are connected by weight vectors. Initially, the weight vectors are initialised with small random numbers and the algorithm calculates the Euclidian distance between an input vector and the weight vector of each output neuron. The neuron with the smallest distance (best-matching unit, BMU) is then selected and the weights from this BMU and the neighbours are updated according to a Gaussian function (Çinar and Merdun, 2009). Nearby neurons in the output layer represents similar properties and neurons located farther away from each other have dissimilar properties (Asan and Ercan, 2012).

The batch training algorithm was used for training the SOM. Firstly, a matrix was organised with the data collect from all cities from March/2020 to January/2021, including the analysed variables. The data set was normalised before the analysis via z-score. Since the discrimination capabilities of the SOM depends on the number of neurons (hexagonal

units) in the maps, several architectures (35 × 35 to 50 × 50) were tested and the most informative one (with the highest discrimination capability) was selected. A summary of the method is displayed in Fig. 2. Maps with a small number of neurons would have the samples clustered together. On the other hand, too big maps would have sample too far apart. Therefore, both high and low number of neurons in the maps would prevent to extraction information and were avoided (Garcia et al., 2007). The software MatLab 2017b (MathWorks, Natick, MA) and the SOM toolbox 2.1 (freely available on http://research.ics.aalto.fi/software/somtoolbox/, accessed in April 2021) were used to perform all analysis (Alhoniemi et al., 2000). The method was also applied to each city separately, testing architectures from 15 × 15 to 25 × 25.

3. Results

Fig. 3 shows the daily variations of the epidemiological and meteorological variables in the studied cities. A descriptive statistical analysis of the epidemiological and meteorological data is presented in Table 1. The results indicate that spatial fluctuations of the meteorological variables were greater than temporal ones (Fig. 3). The T_{avg} for BOG, for instance, varied between 12.9 °C and 15.6 °C (difference of 2.7 °C) from March 2020 to January 2021 (average in the period was 14.1 °C, the lowest among the cities). The difference was much larger (15.0 °C) if BOG is compared with CAR, which presented the highest average of T_{avg} in the study period (29.1 °C) among the cities.

The highest AH values were recorded in the Amazonian (LET) and north coastal cities (BAR and CAR) that presented daily records above 18 g/m^3. In contrast, the capital (BOG) recorded the lowest daily values (maximum AH was 10.2 g/m^3). Regarding WS, the highest values were recorded in the north coastal cities (daily records above 6.8 km/h) and the lowest in LET (maximum WS was 5.9 g/m^3) (Table 1). The h reached the highest daily value (88 kJ/kg) in CAR and the lowest daily value (30.4 kJ/kg) in BOG (Table 1).

A descriptive statistical analysis of the mobility data is presented in Table 2. Moreover, Fig. 4 shows the human mobility data in six place categories in the six cities from Colombia during the analysed period (March 2020–January 2021). The graphs show that these variables were strongly affected by the restriction measures, especially BOG, MED, and BAR. The quarantine appeared to increase the mobility in residential places (RS) in all the cities, standing out BOG that presented average increase of 27.2% (quarantine) when compared to the pre-pandemic period. Conversely, other locations presented a drastic reduction in the number of visitors as a result of the restrictions implemented. While the lowest values for GP, PK, RR, TS and WP were recorded in April 2020, the highest values were in December, exceeding the number of visitors before the quarantine for places such as GP in BOG, MED, CAL and BAR (Fig. 4).

Based on the trends depicted in Fig. 3, the disease dissemination in the country reflected a fast-growing rise from its first detection in March until August 2020. Afterwards, there was downward trend until November. New pronounced peaks occurred in December, likely associated with the year-end celebrations. This motivated the government to implement some restrictions in January again. For our study period, a total of 970,383 confirmed cases were registered in the six cities. BOG was the city with the highest number of NDC (maximum record of 7471 cases in January 2021), followed by CAL and MED (Table 1). Regarding CR, LET had the highest record (396.7 contagions/per 100 thousand people) in May 2020. This city has the lowest urban population density compared to the other assessed cities (Table S1, Appendix A).

3.1. Correlations

The correlations among the epidemiological, meteorological and mobility variables are presented in Table S2 (Appendix A). The results showed that the variables NDC and CR had the same correlations with meteorological and mobility variables. The following relationships were found in the period of quarantine: high correlation correlations involving epidemiological and meteorological variables were obtained between NDC/CR and h, especially in CAL ($r_s = -0.46$, $p < 0.01$) and MED ($r_s = -0.58$, $p < 0.01$). Furthermore, significant negative correlations were found between T_{max}/T_{min}/T_{avg}/AH and NDC/CR in some cities, for example in BOG (T_{max} and T_{avg}: $r_s = -0.62$, $p < 0.01$; AH: $r_s = -0.54$, $p < 0.01$) and CAL (AH: $r_s = -0.53$, $p < 0.01$). In contrast, humidity variables were positively and significantly correlated with NDC/CR in CAR (e.g., AH: $r_s = 0.59$, $p < 0.01$) and BAR (e.g., RH: $r_s = 0.70$, $p < 0.01$). Moreover, the north coastal cities had the highest negative

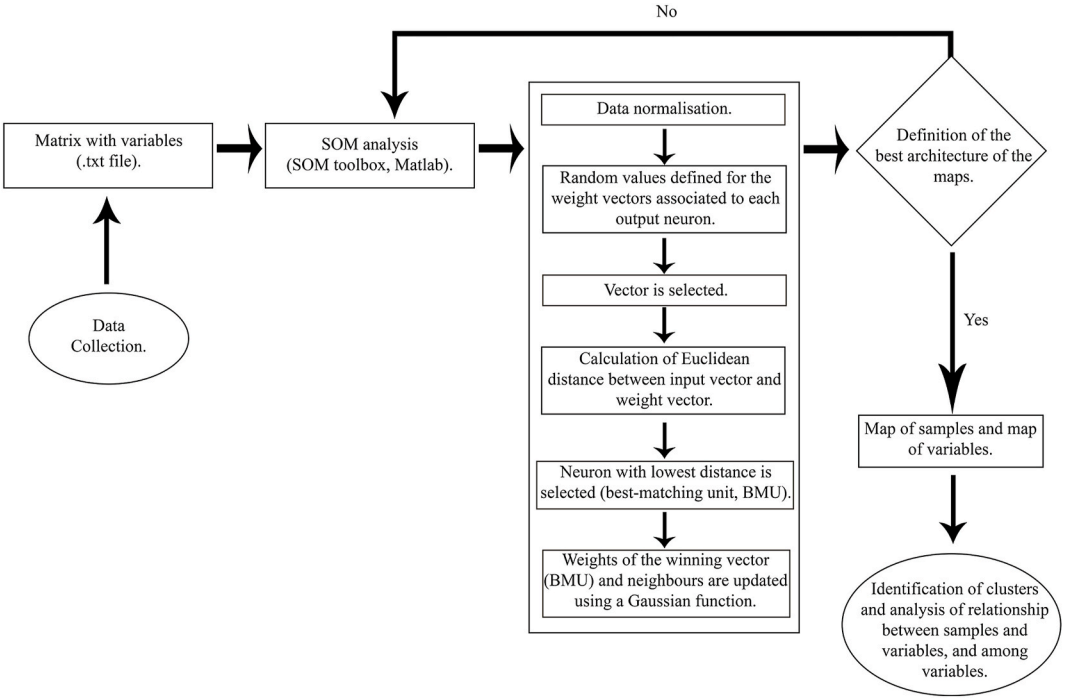

Fig. 2. Flowchart of SOM algorithm application.

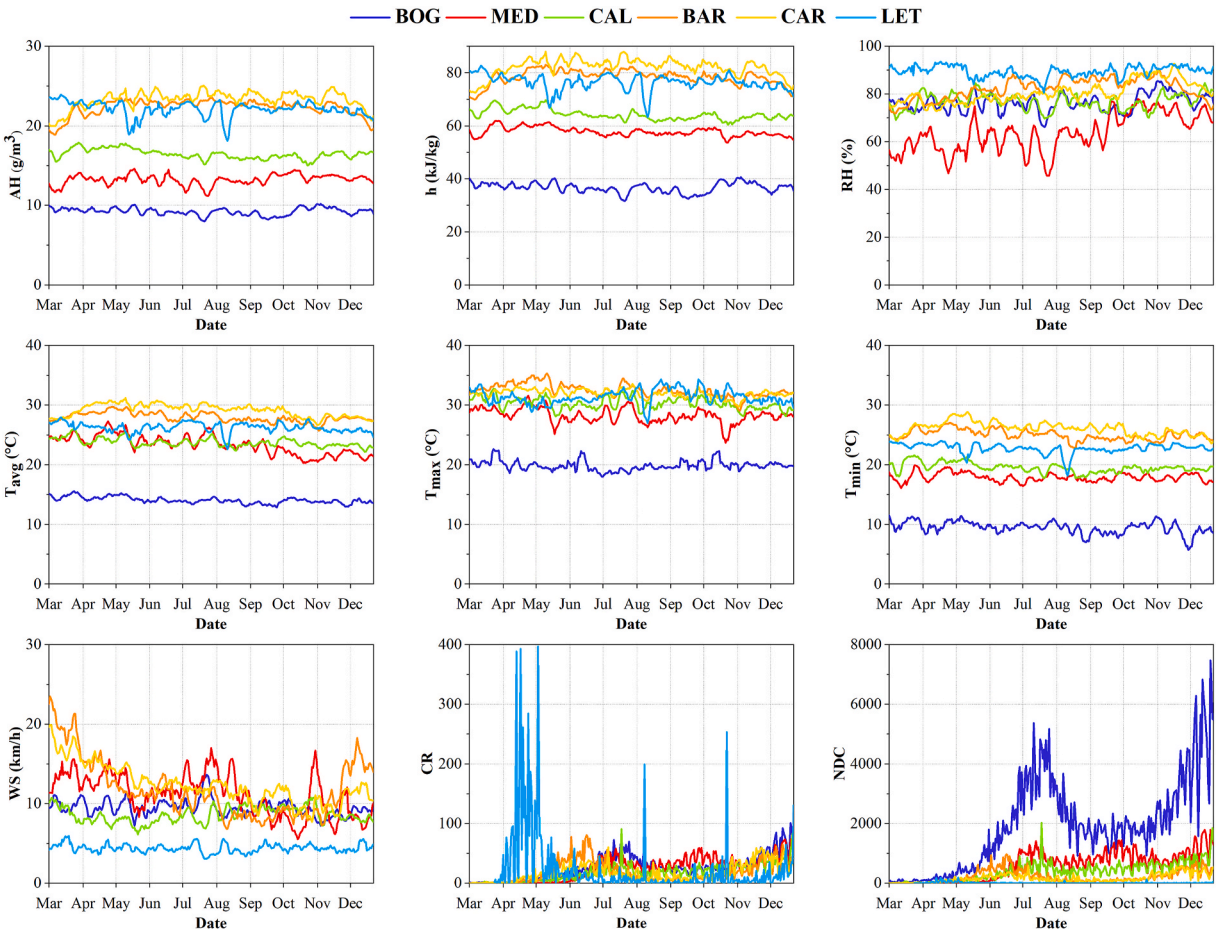

Fig. 3. Meteorological (Average Temperature, Minimum Temperature, Maximum Temperature, Relative Humidity, Absolute Humidity, Wind Speed and Specific Enthalpy) and epidemiological variables (New Daily Cases and Contamination Rate) from March/2020 to January/2021.

coefficients between WS and the epidemiological variables, especially CAR with coefficients (r_s) of −0.70 ($p < 0.01$). Regarding the mobility variables, GP, PK, RR, TS, and WP presented significant positive correlations (except LET) with the epidemiological variables in all the cities. In BOG, MED, and CAL these coefficients (r_s) were higher than the obtained for the meteorological variables. The highest correlations were observed between NDC/CR and PK ($r_s = 0.71$, $p < 0.01$) in CAL and between NDC/CR and RR ($r_s = 0.64$, $p < 0.01$) in BOG. In LET, the mobility variables presented negative coefficients with the epidemiological variables, probably linked with the high caseloads registered in this period.

The period of post-quarantine in cities such as BAR, CAR, and LET presented higher coefficients between the mobility variables and NDC/CR than in the quarantine period (in LET just for PK). Some examples are RR ($r_s = 0.82$, $p < 0.01$) and GP ($r_s = 0.81$, $p < 0.01$) in BAR. In contrast, the most populated cities (BOG, MED and CAL) presented lower coefficients between these variables in post-quarantine than in the quarantine period.

3.2. Self-organising maps

3.2.1. Whole data set

The SOM analysis resulted in 7 groups (I-VI) as shown in the map of samples (Fig. 5). The map architecture 45 × 45 neurons was selected as the most informative one. The neurons were coloured based on the date of the reported confirmed cases (Fig. 5a), the city from where the cases were reported (Fig. 5b), the biome from where the cases were reported (Fig. 5c) and if the data belong to quarantine or post-quarantine period (Fig. 5d). From the figure, it is clear that the data can be clustered using any of these four classifications. The data from the quarantine period (March–August), for instance, were clustered in the bottom-left region, while the data from the post-quarantine period (September–January) were clustered in the upper-right part of the map (Fig. 5d).

Samples located in the same or neighbouring neurons in the map are very similar to each other considering the analysed variables. Conversely, samples in neurons farther from each other are less similar (Brereton, 2012). Therefore, one can say that the data from Bogota (group VII, Fig. 5), for example, are more similar to samples from Medellin (group IV) than data from north coastal cities (BAR and CAR; group I) and Leticia (group III). In contrast, samples from BAR and CAR are very similar because they are very close from each other in the map, belonging to the same groups (groups I and V). This may be linked to the geographical proximity between the cities that share the same biome (subtropical dry forest; Fig. 1). Inside each group, clusters based on the date of the records can also be seen (Fig. 5a). These clusters correspond to temporal stages of the pandemic in each city regarding the analysed variables.

The maps of variables (component planes) are shown in Fig. 6. They are like “hidden” layers behind the map of samples (Fig. 5) and represent the variables used to create the SOM (Brereton, 2012). The colour bars located beside each map represent the intensity of respective variable: the red colour indicates higher intensity and the blue colour lower intensity (Kowalski et al., 2013). From the maps, it is also possible to visualise possible correlations between two variables. GP and RR, for instance, have similar pattern in their maps, indicating a positive correlation. On the other hand, GP and RS have opposite patterns indicating

Table 1
Descriptive statistical analysis of the epidemiological and meteorological variables for each city.

	NDC	CR	T_{max} (°C)	T_{avg} (°C)	T_{min} (°C)	RH (%)	AH (g/m^3)	WS (km/h)	h (kJ/kg)
Bogotá									
Mean	1893.2	25.5	19.9	14.1	9.5	76.4	9.2	9.5	36.7
SD	1533.6	20.7	0.8	0.5	1.0	3.7	0.5	1.0	1.9
CV (%)	81.0	81.0	4.2	3.8	10.9	4.9	4.9	11.0	5.1
Min	9.0	0.1	18.0	12.9	5.7	66.1	8.0	7.2	31.7
Max	7471.0	100.8	22.6	15.6	11.5	85.5	10.2	13.6	41.0
Asym	6.4	6.4	6.5	2.8	−5.4	−0.1	−2.3	7.4	−2.3
Kurt	2.5	2.5	5.2	0.0	4.2	−0.7	−1.8	9.8	−1.0
Medellín									
Mean	582.5	23.2	28.2	23.3	17.9	63.6	13.2	11.2	57.8
SD	480.6	19.8	1.2	1.6	0.5	7.8	0.7	2.6	1.7
CV (%)	82.5	82.5	4.4	6.9	4.0	12.3	5.0	23.5	3.0
Min	0.0	0.0	23.6	20.2	16.1	45.7	11.2	5.5	53.7
Max	1790.0	73.8	31.6	27.3	19.9	77.9	14.6	17.0	61.8
Asym	1.6	1.6	−2.7	0.4	2.5	−0.6	−4.9	−0.9	2.5
Kurt	−3.5	−3.5	4.0	−2.6	−0.3	−2.7	2.1	−3.1	−0.9
Cali									
Mean	393.9	17.7	30.3	23.7	19.5	76.8	16.5	8.6	64.2
SD	314.2	14.1	1.0	0.7	0.8	3.4	0.6	1.0	2.0
CV (%)	79.8	79.8	3.3	3.0	4.2	4.5	3.7	11.7	3.0
Min	0.0	0.0	28.1	22.1	17.7	69.0	15.0	6.1	60.4
Max	2026.0	91.0	32.7	26.0	21.6	84.5	17.9	10.8	70.0
Asym	8.1	8.1	0.6	4.8	2.1	−0.5	1.1	0.9	5.6
Kurt	11.1	11.1	−1.7	1.1	0.0	−2.6	−1.3	−2.6	0.8
Barranquilla									
Mean	217.8	18.1	32.5	28.0	25.0	82.2	22.3	11.8	78.4
SD	216.7	17.9	1.1	0.8	0.9	4.4	1.0	3.7	2.8
CV (%)	99.5	99.5	3.3	2.8	3.5	5.4	4.6	31.3	3.5
Min	0.0	0.0	29.0	25.7	22.7	71.8	18.9	6.8	69.9
Max	972.0	80.6	35.3	29.7	27.0	90.5	23.5	23.5	83.0
Asym	8.8	8.8	0.5	0.2	1.4	−2.8	−11.3	7.2	−7.3
Kurt	3.4	3.4	2.3	−0.8	−1.2	−2.8	7.5	1.7	3.8
Cartagena									
Mean	169.4	17.4	31.9	29.1	26.1	80.6	23.3	12.4	82.0
SD	144.6	14.9	0.7	1.1	1.1	4.5	1.1	2.4	3.3
CV (%)	85.4	85.4	2.2	3.6	4.2	5.6	4.6	19.6	4.0
Min	0.0	0.0	29.7	26.6	23.6	72.8	20.0	7.7	72.6
Max	585.0	60.1	33.6	31.2	28.8	92.7	25.1	19.9	88.0
Asym	7.1	7.1	−3.4	−2.0	1.2	4.6	−8.7	4.6	−7.5
Kurt	0.9	0.9	0.1	−3.8	−0.8	−1.1	5.3	1.1	3.6
Leticia									
Mean	11.4	23.7	31.4	26.2	22.8	89.5	22.1	4.4	76.4
SD	27.2	56.5	1.2	0.8	0.8	2.3	1.0	0.5	3.0
CV (%)	228.8	238.8	3.9	3.1	3.7	2.6	4.4	12.2	3.9
Min	0.0	0.0	27.0	22.6	18.1	80.5	18.1	3.1	63.2
Max	191.0	396.7	34.3	27.9	24.0	93.5	23.9	5.9	83.0
Asym	30.1	30.1	−0.2	−6.8	−15.1	−4.6	−9.8	2.5	−9.1
Kurt	76.4	76.4	1.5	9.2	27.0	1.3	10.4	0.8	11.0

Asym: asymmetry; CV: coefficient of variation; Kurt: kurtosis; Max: maximum value; Min: minimum value; SD: standard deviation.

a negative correlation. Possible associations between epidemiological and meteorological variables can also be found by comparing different variable maps. The neurons with high intensity for CR at the corresponding neurons with lower WS, for instance, indicate that lower WS may favour the virus infections.

The characteristics of each cluster in the map and the similarities and differences among the data can be visualised by simultaneously analysing the map of samples and its component planes. The differences between the quarantine and post-quarantine periods, for instance, can be attributed to the mobility variables GP, PK, RR, TS and WP that presented high intensity for the data from the post-quarantine period (cf. intensity of these variables in Fig. 6 at the position of neurons from post quarantine period as marked in Fig. 5d). The variable RS that presented low intensity during the post-quarantine period also contributed to the formation of both clusters.

Differences among groups can also be explained by visualising the maps of samples and variables. The group VII (BOG samples; Fig. 5), for example, is characterised by low intensities of the meteorological variables AH, h, T_{avg}, T_{max} and T_{min}. Furthermore, the data in this group had the highest NDC. In contrast, groups I, III and V that contains samples from BAR, CAR and LET had high intensities for AH, h, RH, T_{avg}, T_{max} and T_{min}. The main distinction between LET (group III) and the other analysed cities was the lower WS. In addition, the highest CR was recorded for samples from LET.

The SOM analysis indicated that BAR and CAR were the cities that presented the largest differences between quarantine and post-quarantine periods. This is because a substantial amount of data from each period were in different groups (cf. group I with most samples in quarantine period and group V with all samples in post-quarantine period; Fig. 5). The mobility variables (GP, PK, RR, RS, TS and WP) were responsible for the separation of the data in two groups since they presented different intensities in each analysed group. In the same way, these variables were also responsible for dividing CAL data into two groups (II and VI, Fig. 5).

3.2.2. SOM by city

The maps of samples of each city individually were coloured and grouped based on the date of the reported infections (Fig. S1, Appendix

Table 2
Descriptive statistical analysis of the mobility variables for each city.

	PK	WP	TS	RR	GP	RS
	(Δ%)	(Δ%)	(Δ%)	(Δ%)	(Δ%)	(Δ%)
Bogotá						
Mean	−40.8	−40.2	−45.2	−51.9	−23.0	22.9
SD	15.3	16.6	21.8	16.1	18.1	8.7
CV (%)	−37.6	−41.2	−48.3	−31.1	−78.7	37.9
Min	−77.9	−70.9	−81.9	−85.1	−62.0	3.0
Max	−7.0	5.1	0.4	10.4	18.9	40.1
Asym	−5.2	3.8	1.5	−1.4	−1.7	1.9
Kurt	0.1	0.4	−3.4	−1.3	−1.2	−2.9
Medellín						
Mean	−41.9	−35.9	−48.4	−49.7	−26.9	18.3
SD	16.8	18.4	18.2	19.9	21.2	8.0
CV (%)	−40.1	−51.1	−37.6	−40.0	−78.9	43.8
Min	−80.1	−77.3	−82.7	−87.7	−68.0	2.7
Max	−11.4	1.7	7.4	10.3	19.3	35.0
Asym	−5.3	−5.0	−0.8	−1.4	−1.3	3.6
Kurt	−1.1	−0.8	−2.3	−2.7	−2.6	−2.3
Cali						
Mean	−42.0	−30.9	−36.5	−43.5	−19.6	16.2
SD	17.3	18.1	18.6	19.3	19.8	7.6
CV (%)	−41.2	−58.8	−50.8	−44.4	−101.4	46.8
Min	−82.0	−74.0	−76.6	−84.4	−63.3	−1.6
Max	8.9	5.0	3.3	9.7	17.3	33.0
Asym	−7.3	−6.6	−3.8	−4.4	−4.4	5.2
Kurt	−0.3	0.3	−1.4	−2.0	−1.6	−1.5
Barranquilla						
Mean	−48.6	−38.9	−51.2	−54.2	−28.0	19.1
SD	20.1	18.6	22.1	19.6	25.2	6.8
CV (%)	−41.3	−46.5	−43.2	−36.1	−90.2	35.6
Min	−81.9	−76.1	−81.3	−85.0	−67.1	1.3
Max	−5.0	5.7	0.1	−9.3	29.0	30.9
Asym	0.5	−0.9	2.9	1.4	1.5	−0.3
Kurt	−4.0	−3.4	−3.8	−4.1	−4.7	−4.3
Cartagena						
Mean	−68.1	−42.7	−71.1	−62.6	−38.7	19.0
SD	14.8	17.0	16.7	16.2	22.2	6.2
CV (%)	−21.7	−39.9	−23.5	−25.9	−57.3	32.4
Min	−88.9	−74.3	−91.3	−86.6	−72.6	2.9
Max	−30.6	1.7	−17.0	−19.0	7.1	29.6
Asym	3.1	−1.0	5.2	2.9	1.6	−0.2
Kurt	−3.5	−3.5	−2.3	−3.4	−4.4	−4.2
Leticia						
Mean	−55.9	−20.4	NA	NA	NA	NA
SD	13.6	16.4	NA	NA	NA	NA
CV (%)	−24.3	−80.3	NA	NA	NA	NA
Min	−80.3	−49.6	NA	NA	NA	NA
Max	−12.0	8.0	NA	NA	NA	NA
Asym	1.8	−2.0	NA	NA	NA	NA
Kurt	0.6	−3.6	NA	NA	NA	NA

Asym: asymmetry; CV: coefficient of variation; Kurt: kurtosis; NA: not available; Max: maximum value; Min: minimum value; SD: standard deviation.

A). They were classified in 4 (I-IV) or 5 (I–V) groups, from where it is possible to visualise the influence of restriction measures: the groups from March to August/2020 (quarantine) are in one side of the maps and the groups from September/2020 to January/2021 (post-quarantine) are in the other sited of the maps. From the component planes of each city (Fig. S2-27, Appendix A), the mobility variables (GP, PK, RR, RS, TS and WP) were responsible for the distinctions between these two periods in all cities individually. Apart from RS, these variables presented higher intensities in the post-quarantine, indicating that they had higher importance during this period. In contrast, RS presented the highest intensity and importance during the quarantine months.

The analysis of the component planes (Figs. S2–S7, Appendix A) showed that the relationship between epidemiological and meteorological variables presented distinct trends during quarantine. The maps from BAR, CAR and LET (Fig. S2, S5 and S6, Appendix A), for instance, revealed that days with higher number of new cases (high NDC and CR) had higher intensities for AH and h. WS presented the opposite trend (higher WS, lower number of cases), except for LET where this association is not clear. The maps from CAL and MED (Figs. S4 and S7, Appendix A) showed that low records of T_{min} were related to high NDC/CR values. On the other hand, high NDC/CR was related in BOG to lower T_{avg} and T_{max} (Fig. S3, Appendix A). In BOG and CAL (Figs. S3 and S4, Appendix A) days with high intensities for NDC/CR had lower values of AH, RH and h.

No clear patterns could be visualised in the post-quarantine period between epidemiological and meteorological variables in most component planes (Fig. S2 – Fig. S7, Appendix A). In CAL, for example, the highest number of NDC/CR was related to a lower T_{avg} and T_{max}. These maps also show that mobility variables in post-quarantine were dominant and well correlated with epidemiological variable in most of the cities (e.g., the neurons with highest intensity for GP, PK, RR, TS and WP in CAR maps were related to neurons with highest intensity for NDC/CR. Fig. S5, Appendix A).

4. Discussion

The dynamics of SARS-CoV-2 in Colombia appear to be affected by the different biomes in the country as revealed by the clusters visualised in SOM analysis (Fig. 5c). This is supported by Kubota et al. (2020) who speculated that specific factors (e.g., weather) from different biogeographic regions affect partially the development of the pandemic. Since the weather is considered a modulator of the stability or inhibition of SARS-CoV-2, the particular meteorological conditions of each city may have influenced the differences in the outbreaks (Briz-Redón and Serrano-Aroca, 2020a; Oliveiros et al., 2020; Paraskevis et al., 2021). Although, environmental conditions are not the single driver of the COVID-19 spread and other important factors (e.g., socioeconomic conditions, immunity, etc.) that were not considered in this study could have had a relevant role in the mechanism of transmission (Kubota et al., 2020; Wei et al., 2020). Furthermore, the samples were clearly divided by period (quarantine and post-quarantine, Fig. 5d) which support the effects of the containment measures. Indeed, independently of the climate of each city, isolation restrictions decrease the impact of the COVID-19 outbreaks (Maier and Brockmann, 2020).

In the quarantine period, the meteorological variables reflected clearer relationships with the caseloads than in the post-quarantine period. The lower effect of weather in the post-quarantine may be related to the increment of human mobility, since social contact rises the probability of contracting COVID-19 (Fazio et al., 2021). In addition, the increase of contagions in our study may be explained by different combinations of two or more meteorological conditions (e.g., higher NDC/CR were associated with lower AH, h and T_{min} in CAL). This is supported by other studies which reported that the analysis of just a single variable is not enough to explain the dynamics of the virus (Bannister-Tyrrell et al., 2020; Beggs and Avital, 2021; Chen et al., 2020). Auler et al. (2020), for instance, found that a combination of RH around 80% and T_{avg} of 27.5 °C may explain the evolution of COVID-19 in some cities in Brazil.

Our findings revealed distinct effects of temperature (T_{avg}, T_{max} and T_{min}) and humidity (AH and RH) variables on the COVID-19 spread in the assessed cities. It corroborates the adaptability of this new coronavirus to different environmental conditions (Bhardwaj and Agrawal, 2020; Yang et al., 2021). In MED and CAL, when T_{min} was lower (<18 °C and <17 °C, respectively) the number of contagions increased in quarantine (Figs. S4 and S7, Appendix A). This trend was also verified in other countries as Spain or China (Fernández-Ahúja and Martínez, 2021; Yang et al., 2021). In the case of T_{max}, this variable has been negatively correlated with the COVID-19 infections in cities as Wuhan (China) (Yang et al., 2021). In our study, BOG registered an increase of cases when T_{max} was below 20 °C in quarantine (Fig. S3, Appendix A). Other negative associations in this city were related to T_{avg} and AH with the contagions, especially when these variables were lower than 14 °C and 9 g/m^3, respectively (Fig. S3, Appendix A). This agrees with other epidemiological studies with this novel coronavirus and its predecessors

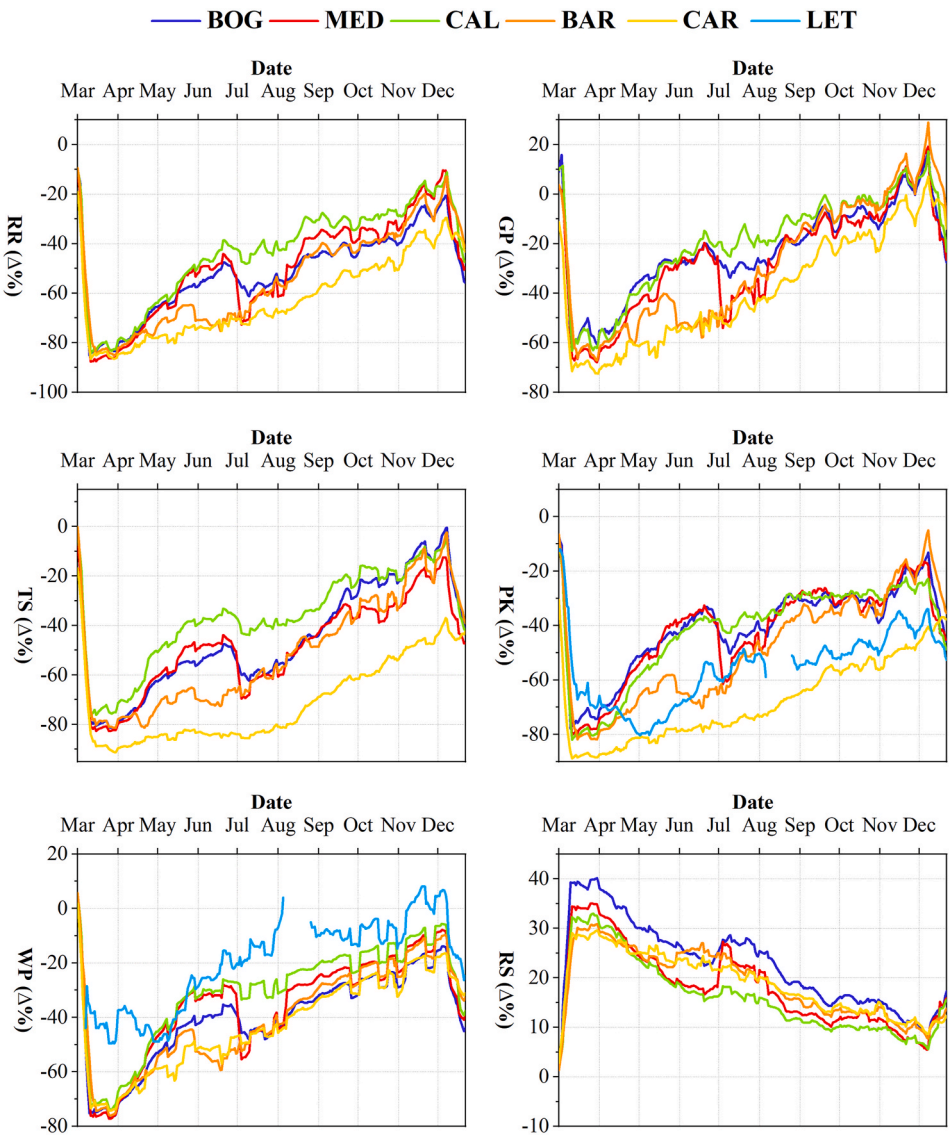

Fig. 4. Mobility variables (Retail and Recreation, Grocery and Pharmacy, Parks, Transport Stations, Workplaces, and Residential) from March/2020 to January/2021.

suggesting a higher transmission when temperature and humidity decrease (Briz-Redón and Serrano-Aroca, 2020a; Chan et al., 2011; Fernández-Ahúja and Martínez, 2021; Gardner et al., 2019; Nottmeyer and Sera, 2021). The stability of the virus in cold temperatures is associated to its heat intolerance (Beggs and Avital, 2021). Furthermore, colder/drier conditions such as the ones observed in BOG may promote that the respiratory droplets with the virus continue suspended for more time (Wang et al., 2021). These settings dry out the human mucous membrane, reducing the function of cilia and supporting the transmission of the disease (Qi et al., 2020; Sun et al., 2020). Some BOG records for T_{avg} (12.9–15.6 °C; Table 1) and AH (8–10.2 g/m^3; Table 1) corresponded with the vulnerable ranges to the virus spread reported in the literature: 4–9 g/m^3 and 3–17 °C (Bukhari and Jameel, 2020), 3–8 g/m^3 and 5–11 °C (Sajadi et al., 2020), 4–6 g/m^3 and 4–11 °C (Gupta et al., 2020). However, other demographic factors (Table S1, Appendix A) must be taking into consideration, for instance, the high population density may increase the frequency of direct contact (Diao et al., 2021; Lin et al., 2020). This is relevant if it is considered that BOG and MED have been listed as cities with the most higher and concentrated densities in the world (Brodie, 2017; Burdett, 2015; Wheeler, 2015).

In the case of the hottest (average $T_{avg} > 26$ °C) and wettest (average AH > 22 g/m^3) cities of the study, the increase of AH (BAR, CAR and LET) and T_{avg} (CAR) were related to higher NDC/CR records (Fig. S2, S5 and S6, Appendix A). Although high T_{avg} favour the instability of the virus in suspended droplets, it increments the amount of virus settled on surfaces (Magurano et al., 2021). Moreover, the likelihood of SARS-CoV-2 survival is approximately five times higher under humid conditions than under dry conditions, which may have influenced the contagions in these cities (Bhardwaj and Agrawal, 2020). The mechanisms of transmission of respiratory viruses in hot-wet settings seems to be related to: (i.) fomites, due to the faster deposition of virus-laden droplets on surfaces and their slow evaporation (Paynter, 2015; Rodó et al., 2021); (ii.) direct contact through small virus-laden particles produced by air conditioner systems (Ahlawat et al., 2020).

Humid-rainy conditions in Colombia have been associated with outbreaks of other respiratory viruses such as influenza and respiratory syncytial virus (RSV) (Gamba-Sanchez et al., 2016; Rodriguez-Martinez et al., 2015; Tamerius et al., 2013). This agrees with our data that show that COVID-19 outbreaks occurred in BAR, CAR and LET under wet conditions (average AH > 22 g/m^3). Moreover, our results accord with the hypothesis proposed by Auler et al. (2020): the reduction in CR associated with high temperature and humidity is not entirely reliable

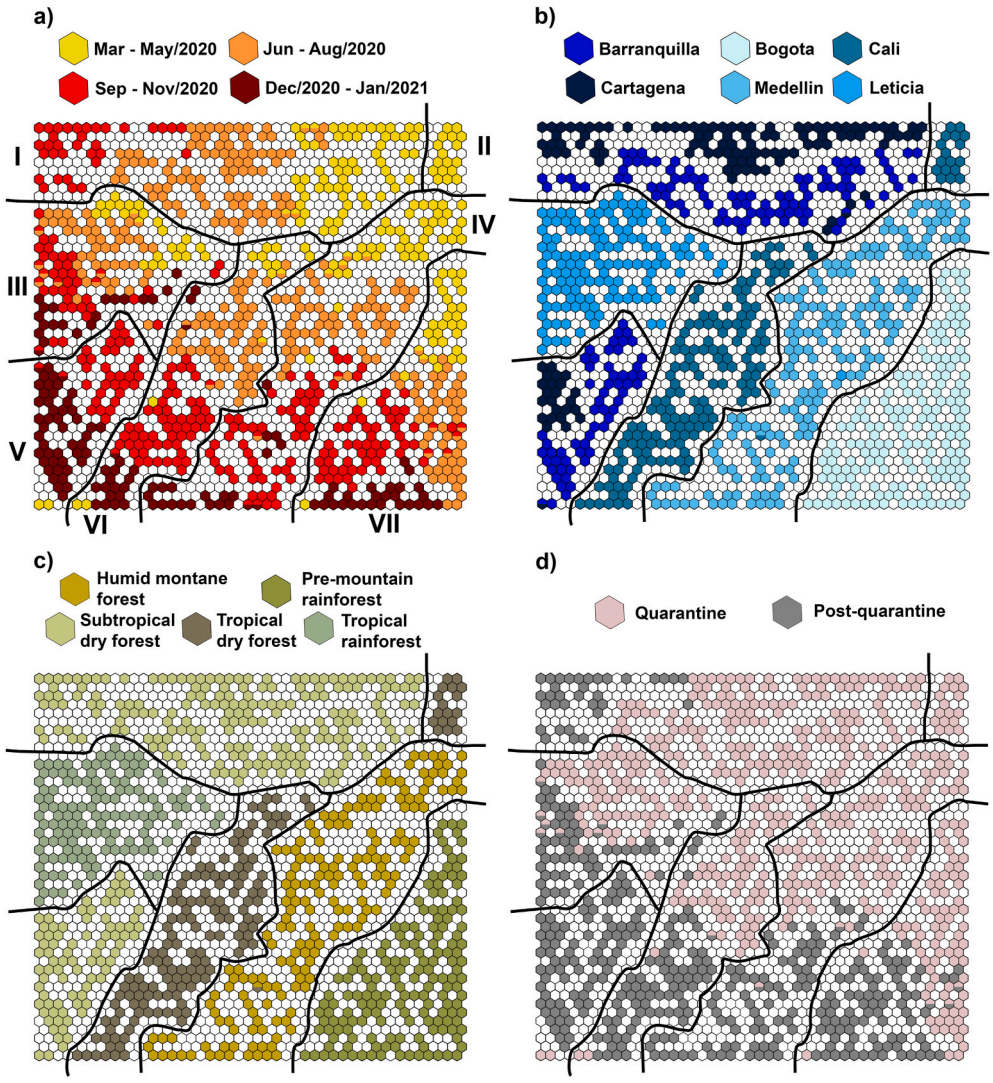

Fig. 5. Map of samples of the whole dataset classified by date of the reported cases (a), the city from where the cases were reported (b), the biome from where the cases where reported (c), and the period to which the data belongs (d). The samples were divided in 7 distinct groups (I-VII) based on the proximity between samples in the neurons (hexagonal units) and the different classifications.

for cities in tropical and subtropical regions. This conclusion is supported by other authors as Raines et al. (2020), who also identified in CAR a considerable increment of NDC in quarantine that was correlated with a RH above 78%. Likewise, Prata et al. (2021) found in Brazil that each 1% rise of the daily RH is associated with increments in COVID-19 cases of 2.26% in tropical regions and 2.35% in subtropical regions.

Special attention deserves h because it includes the effect of two variables at the same time (T_{avg} and RH). Some studies have listed h as a significant predictor variable of the SARS-CoV-2 survival (Beggs and Avital, 2021; Spena et al., 2020a). In our case, this variable for cities such as BOG, MED and CAL presented even higher correlation coefficients (Table S2, Appendix A) and clearer patterns with NDC/CR (e.g., Figs. S2 and S3, Appendix A) than temperature (T_{avg}, T_{max} and T_{min}) or humidity (AH and RH) variables, particularly in the quarantine period. Spena and collaborators (2020b) proposed a seasonal virulence risk scale based on the incidence rate of COVID-19 and h. This scale set a negligible risk when $h < 9$ kJ/kg and when $h > 33$ kJ/kg; low-to-average risk when h is between 9 and 12 kJ/kg and when h is between 23 and 33 kJ/kg; and average-to-high risk when h is between 12 and 23 kJ/kg. In our study, all assessed cities were classified as negligible risk, except BOG that presented potential risk (low-to-average risk) considering its h records (h between 30.4 and 36.4 kJ/kg, Table 1). It is consistent with our findings since BOG presented the highest NDC records throughout the study (maximum value of 7471 cases). However, cities that registered high CR values (BAR, CAR and LET) were not classified as average-to-high potential risk in the scale. Consequently, it is necessary to include the conditions of cities in (sub)tropical regions and the possible effect of other modulator variables (e.g., WS in LET) in this type of scale (which is based on temperate regions).

Regarding WS, it can modulate the dynamics of SARS-CoV-2 by reducing the suspending time of the virus in the air due to dilution and consequent removal (Ahmadi et al., 2020; N. Islam et al., 2020; Wang et al., 2021). This can be seen in the north coastal cities where the high WS records were related to diminutions in the caseloads (especially in the quarantine period, Figs. S2 and S5, Appendix A). The potential of WS to gradually reduce the effects of the pandemic also has been observed in other tropical coastal cities like Rio de Janeiro (Brazil) (Rosario et al., 2020). On the other hand, some studies determined higher contagion rates when the WS values were below 5.4 km/h in China (Wei et al., 2020) and 7.2 km/h in Italy (Coccia, 2020). In this investigation, the city (LET) with more records below these limits presented the highest CRs (Fig. 3; Table 1). This suggests that this variable may be an important factor controlling the virus transmission across Colombia.

Concerning the mobility variables, when people spent more time at

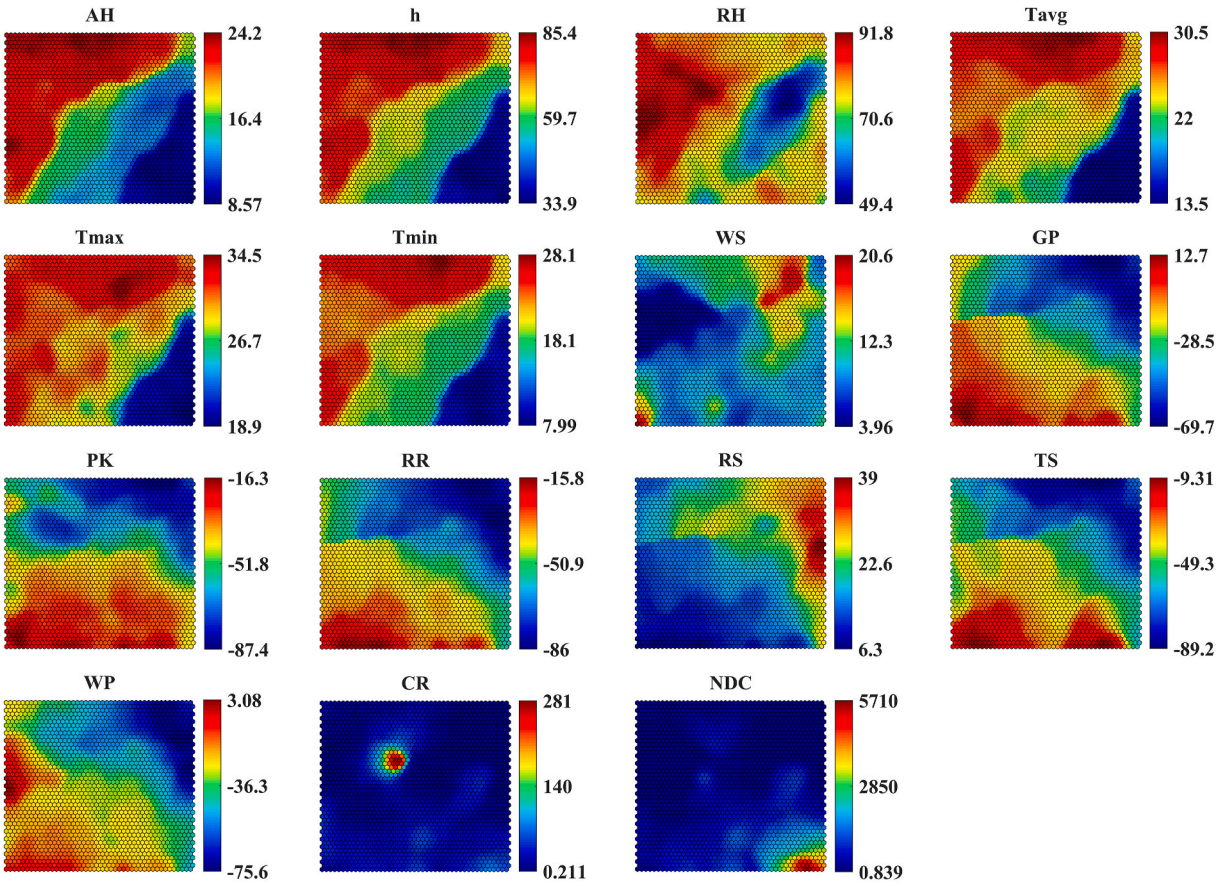

Fig. 6. Maps of variables of the whole dataset (component planes). The colour bar beside each map indicates the intensity of the variable: the red colour indicates high intensity and blue colour indicates low intensity. (For interpretation of the references to colour in this figure legend, the reader is referred to the Web version of this article.)

home (residential mobility), the transmission of SARS-CoV-2 was lower compared to the other variables (GP, PK, RR, TS, and WP). Previous studies stressed on the implications of weather on human interactions, for instance, warmed days may be associated with outdoor activities (e.g., visits to parks or public places) and more exposure to the virus (Damette et al., 2021; Shao et al., 2021). This is evident in our study in cities as BAR and CAR with clear patterns in post-quarantine between the mobility and epidemiological variables. A study developed at Johns Hopkins University revealed significant associations among the SARS-CoV-2 infections, the use of public transport, gatherings with more than 10 people and more than 100 people, and visits to indoor or outdoor places with crowds (Clipman et al., 2020). Finally, the role of mobility variables on the increment of cases in the post-quarantine period mirrored that the lockdown is a sensible alternative but an effective way to control the transmission of SARS-CoV-2. It has been evidenced in studies carried out in China, England or Italy (Cartenì et al., 2020; Chinazzi et al., 2020; Sartorius et al., 2021; Vollmer et al., 2020; Y. Zhou et al., 2020).

Our findings are limited by the socioeconomic conditions of the country, e.g., Colombia has a Human Development Index of 0.74 (http://hdr.undp.org, accessed in April 2021) with serious gaps in the provision of health and food services that could easily counteract any potential climatic effect at local scales (Coelho et al., 2020). In addition, this investigation did not take into consideration other possible predictors as the number of tests applied, general health policies, transportation or cultural aspects (Oliveiros et al., 2020). However, we considered that our results may contribute to a better understanding of how SARS-CoV-2 is sustained in tropical countries such as Colombia. In addition, other strengths are: (i.) the evaluation of 15 different variables using a dataset of 10 months, unlike several studies that assessed narrower periods (Sanchez-Lorenzo et al., 2021; Yang et al., 2021); (ii). This study about the influence of multiple variables (meteorological and mobility) on the SARS-CoV-2 transmission in Colombia could be carried out using other methods such as Principal Component Analysis (PCA) or Partial Least Squares (PLS). Nevertheless, the use of SOM technique presents several advantages related to its highlighted visualisation capabilities with different graphical representation options, its good performance in clustering and pattern recognition, efficient use of space in the maps and its robustness to missing data or noise (Brereton, 2012; Gontijo et al., 2021).

5. Conclusions

This study has shown that different biogeographical regions in Colombia had distinct dynamics regarding the virus spread. This was attributed to both restriction measures that affected human mobility and larger spatial than temporal variations of the analysed meteorological variables. Hence, our outcomes may contribute to the implementation of measures to preserve public health and the formulation of site-specific policies to prevent disease dissemination.

The highest CR occurred in LET, where the lowest WS may have an important influence on the virus transmission. In MED and CAL, T_{min} had an important role in the increment of NDC/CR. Furthermore, the highest NDC recorded in BOG appeared to be linked to a decrease in T_{avg} (<14 °C) and AH (<9 g/m^3), besides its largest population, higher population density and importance. The increase of AH and T_{avg} also seemed to favour the virus spread in warmer and wetter cities with an average $T_{avg} > 26.2$ °C and AH > 22.1 g/m^3 (BAR, CAR and LET) that

achieved higher CR records. The different impact of meteorological variables on the virus transmission may be connected to local characteristics such as sociodemographic aspects and combined factors.

The human mobility variables influenced the development of the pandemic in most of the analysed cities, especially in the post-quarantine period. The higher amount of time spent at home was more important when quarantine was in place. This supported the efficacy of the restriction measures during quarantine, when meteorological variables seem to have grown in importance These measures did not avoid a fast spread of the virus (e.g., in LET), supporting the need for well-ventilated spaces, stricter hygiene and restriction measures, and investigation of other variables (e.g., solar radiation, air pollutants or vaccination rate).

The SOM analysis was suitable to show the distinctions between quarantine and post-quarantine periods, differences related to local biomes (e.g., humidity effects) and the development of the pandemic considering all analysed variables combined. This technique can be applied in other regions based on its ability to spatially or temporally group samples. Future investigations using SOM should focus on (i.) comparing the specific conditions (e.g., weather or mobility) of regions located in other latitudes and their implemented strategies to cope with the pandemic; (ii.) assessing the dynamic of the new virus variants and whether the meteorological conditions have the same influence; (iii.) (sub)tropical regions, especially in Latin America or Africa, where the influence of particular environmental (e.g., high humidity did not prevent the increase of contagions in this study), socioeconomic (e.g., access to healthcare or migration) or sanitary (e.g., drinking water) conditions on the pandemic needing more attention (Briz-Redón and Serrano-Aroca, 2020b).

Declaration of competing interest

The authors declared no conflict of interests.

Acknowledgements

S. Gómez-Herrera and S. Enríquez-Delgado thank the support of the government of Nariño (Colombia) and Ceiba Foundation for the scholarships granted. E. S. J Gontijo and A. H Rosa would like to thank the São Paulo Research Foundation (FAPESP, grant number 19/06800–5) and the Coordination for the Improvement of Higher Education Personnel (CAPES, grant number 99999.008107/2015–07) for financial support.

Appendix A. Supplementary data

Supplementary data to this article can be found online at https://doi.org/10.1016/j.ijheh.2021.113833.

References

Aboubakr, H.A., Sharafeldin, T.A., Goyal, S.M., 2020. Stability of SARS-CoV-2 and other coronaviruses in the environment and on common touch surfaces and the influence of climatic conditions: a review. Transbound Emerg. Dis. 68, 296–312. https://doi.org/10.1111/tbed.13707.

Ahlawat, A., Wiedensohler, A., Mishra, S.K., 2020. An overview on the role of relative humidity in airborne transmission of SARS-CoV-2 in indoor environments. Aerosol. Air Qual. Res. 20, 1856–1861. https://doi.org/10.4209/aaqr.2020.06.0302.

Ahmadi, M., Sharifi, A., Dorosti, S., Jafarzadeh Ghoushchi, S., Ghanbari, N., 2020. Investigation of effective climatology parameters on COVID-19 outbreak in Iran. Sci. Total Environ. 729, 138705. https://doi.org/10.1016/j.scitotenv.2020.138705.

Alduchov, O.A., Eskridge, R.E., 1996. Improved magnus form approximation of saturation vapor pressure. J. Appl. Meteorol. Climatol. 35, 601–609. https://doi.org/10.1175/1520-0450(1996)035<0601:IMFAOS>2.0.CO, 2.

Alhoniemi, E., Himberg, J., Parhankangas, J., Vesanto, J., 2000. SOM Toolbox for Matlab. SOM Toolbox Team. Helsinki University, Espoo.

Araújo, M.B., Naimi, B., 2020. Spread of SARS-CoV-2 Coronavirus likely constrained by climate. medRxiv. https://doi.org/10.1101/2020.03.12.20034728, 03.12.20034728.

Arellana, J., Márquez, L., Cantillo, V., 2020. COVID-19 outbreak in Colombia: an analysis of its impacts on transport systems [WWW Document]. Journal of Advanced Transportation. https://doi.org/10.1155/2020/8867316.

Asan, U., Ercan, S., 2012. An introduction to self-organizing maps. Computational Intelligence Systems in Industrial Engineering. Springer, pp. 295–315.

Auler, A.C., Cássaro, F.A.M., da Silva, V.O., Pires, L.F., 2020. Evidence that high temperatures and intermediate relative humidity might favor the spread of COVID-19 in tropical climate: a case study for the most affected Brazilian cities. Sci. Total Environ. 729, 139090. https://doi.org/10.1016/j.scitotenv.2020.139090.

Bannister-Tyrrell, M., Meyer, A., Faverjon, C., Cameron, A., 2020. Preliminary evidence that higher temperatures are associated with lower incidence of COVID-19, for cases reported globally up to 29th February 2020. medRxiv. https://doi.org/10.1101/2020.03.18.20036731, 03.18.20036731.

Battineni, G., Chintalapudi, N., Amenta, F., 2020. Tropical Conditions and Outbreak of COVID-19. Pharmaceutical and Biomedical Research.

Beggs, C.B., Avital, E.J., 2021. A psychrometric model to assess the biological decay of the SARS-CoV-2 virus in aerosols. PeerJ 9, e11024.

Berberan-Santos, M.N., Bodunov, E.N., Pogliani, L., 1997. On the barometric formula. Am. J. Phys. 65, 404–412. https://doi.org/10.1119/1.18555.

Bhardwaj, R., Agrawal, A., 2020. Likelihood of survival of coronavirus in a respiratory droplet deposited on a solid surface. Phys. Fluids 32, 061704. https://doi.org/10.1063/5.0012009.

Bochenek, B., Jankowski, M., Gruszczynska, M., Nykiel, G., Gruszczynski, M., Jaczewski, A., Ziemianski, M., Pyrc, R., Figurski, M., Pinkas, J., 2021. Impact of meteorological conditions on the dynamics of the COVID-19 pandemic in Poland. Int. J. Environ. Res. Publ. Health 18, 3951.

Brereton, R.G., 2012. Self organising maps for visualising and modelling. Chem. Cent. J. 6, S1. https://doi.org/10.1186/1752-153X-6-S2-S1.

Briz-Redón, Á., Serrano-Aroca, Á., 2020a. The effect of climate on the spread of the COVID-19 pandemic: a review of findings, and statistical and modelling techniques. Prog. Phys. Geogr.: Earth Environ. 44, 591–604.

Briz-Redón, Á., Serrano-Aroca, Á., 2020b. A spatio-temporal analysis for exploring the effect of temperature on COVID-19 early evolution in Spain. Sci. Total Environ. 728, 138811. https://doi.org/10.1016/j.scitotenv.2020.138811.

Brodie, C., 2017. These Are the World's Most Crowded Cities. Presented at the World Economic Forum.

Bukhari, Q., Jameel, Y., 2020. Will coronavirus pandemic diminish by summer? SSRN J. https://doi.org/10.2139/ssrn.3556998.

Burdett, R., 2015. A Tale of Four World cities–London, Delhi, Tokyo and Bogotá Compared, vol. 11. The Guardian.

Car, Z., Baressi Šegota, S., Anđelić, N., Lorencin, I., Mrzljak, V., 2020. Modeling the spread of COVID-19 infection using a multilayer perceptron. Comput. Math. Methods Med. 2020, 1–10. https://doi.org/10.1155/2020/5714714.

Cartenì, A., Di Francesco, L., Martino, M., 2020. How mobility habits influenced the spread of the COVID-19 pandemic: results from the Italian case study. Sci. Total Environ. 741, 140489.

Chan, K.H., Peiris, J.S.M., Lam, S.Y., Poon, L.L.M., Yuen, K.Y., Seto, W.H., 2011. The effects of temperature and relative humidity on the viability of the SARS coronavirus. Adv. Virol. 734690. https://doi.org/10.1155/2011/734690.

Chen, B., Liang, H., Yuan, X., Hu, Y., Xu, M., Zhao, Y., Zhang, B., Tian, F., Zhu, X., 2020. Roles of Meteorological Conditions in COVID-19 Transmission on a Worldwide Scale (Preprint). Infectious Diseases (Except HIV/AIDS). https://doi.org/10.1101/2020.03.16.20037168.

Chinazzi, M., Davis, J.T., Ajelli, M., Gioannini, C., Litvinova, M., Merler, S., Piontti, A.P. y, Mu, K., Rossi, L., Sun, K., Viboud, C., Xiong, X., Yu, H., Halloran, M.E., Longini, I. M., Vespignani, A., 2020. The effect of travel restrictions on the spread of the 2019 novel coronavirus (COVID-19) outbreak. Science 368, 395–400. https://doi.org/10.1126/science.aba9757.

Çinar, Ö., Merdun, H., 2009. Application of an unsupervised artificial neural network technique to multivariant surface water quality data. Ecol. Res. 24, 163–173.

Clipman, S.J., Wesolowski, A.P., Gibson, D.G., Agarwal, S., Lambrou, A.S., Kirk, G.D., Labrique, A.B., Mehta, S.H., Solomon, S.S., 2020. Rapid Real-Time Tracking of Nonpharmaceutical Interventions and Their Association with Severe Acute Respiratory Syndrome Coronavirus 2 (SARS-CoV-2) Positivity: the Coronavirus Disease 2019 (COVID-19) Pandemic Pulse Study. Clinical Infectious Diseases. https://doi.org/10.1093/cid/ciaa1313.

Coccia, M., 2020. Factors determining the diffusion of COVID-19 and suggested strategy to prevent future accelerated viral infectivity similar to COVID. Sci. Total Environ. 729, 138474. https://doi.org/10.1016/j.scitotenv.2020.138474.

Coelho, M.T.P., Rodrigues, J.F.M., Medina, A.M., Scalco, P., Terribile, L.C., Vilela, B., Diniz-Filho, J.A.F., Dobrovolski, R., 2020. Global expansion of COVID-19 pandemic is driven by population size and airport connections. PeerJ 8, e9708. https://doi.org/10.7717/peerj.9708.

Coşkun, H., Yıldırım, N., Gündüz, S., 2021. The spread of COVID-19 virus through population density and wind in Turkey cities. Sci. Total Environ. 751, 141663. https://doi.org/10.1016/j.scitotenv.2020.141663.

Damette, O., Mathonnat, C., Goutte, S., 2021. Meteorological factors against COVID-19 and the role of human mobility. PloS One 16, e0252405. https://doi.org/10.1371/journal.pone.0252405.

de Castro Júnior, S.L., da Silva, I.J.O., 2021. The specific enthalpy of air as an indicator of heat stress in livestock animals. Int. J. Biometeorol. 65, 149–161. https://doi.org/10.1007/s00484-020-02022-8.

De la Hoz-Restrepo, F., Alvis-Zakzuk, N.J., De la Hoz-Gomez, J.F., De la Hoz, A., Gómez Del Corral, L., Alvis-Guzmán, N., 2020. Is Colombia an example of successful containment of the 2020 COVID-19 pandemic? A critical analysis of the epidemiological data, March to July 2020. International Journal of Infectious Diseases 99, 522–529. https://doi.org/10.1016/j.ijid.2020.08.017.

Departamento Administrativo Nacional de Estadistica, 2018. Censo nacional de Población y vivienda 2018 [WWW Document]. URL. https://www.dane.gov.co/in

dex.php/estadisticas-por-tema/demografia-y-poblacion/censo-nacional-de-poblacion-y-vivenda-2018, 11,22,20.
Dhand, R., Li, J., 2020. Coughs and sneezes: their role in transmission of respiratory viral infections, including SARS-CoV-2. Am. J. Respir. Crit. Care Med. 202, 651–659. https://doi.org/10.1164/rccm.202004-1263PP.
Dhouib, W., Maatoug, J., Ayouni, I., Zammit, N., Ghammem, R., Fredj, S.B., Ghannem, H., 2021. The incubation period during the pandemic of COVID-19: a systematic review and meta-analysis. Syst. Rev. 10, 101. https://doi.org/10.1186/s13643-021-01648-y.
Diao, Y., Kodera, S., Anzai, D., Gomez-Tames, J., Rashed, E.A., Hirata, A., 2021. Influence of population density, temperature, and absolute humidity on spread and decay durations of COVID-19: a comparative study of scenarios in China, England, Germany, and Japan. One Health 12, 100203. https://doi.org/10.1016/j.onehlt.2020.100203.
Doan, Q.-V., Kusaka, H., Sato, T., Chen, F., 2020. A structural self-organizing map (S-SOM) algorithm for weather typing. Geosci. Model Dev. Discuss. (GMDD) 1–27.
Farkas, C., Iclanzan, D., Olteán-Péter, B., Vekov, G., 2021. Estimation of parameters for a humidity-dependent compartmental model of the COVID-19 outbreak. PeerJ 9, e10790. https://doi.org/10.7717/peerj.10790.
Fazio, R.H., Ruisch, B.C., Moore, C.A., Samayoa, J.A.G., Boggs, S.T., Ladanyi, J.T., 2021. Social distancing decreases an individual's likelihood of contracting COVID-19. Proc. Natl. Acad. Sci. Unit. States Am. 118 https://doi.org/10.1073/pnas.2023131118.
Fernández-Ahúja, J.M.L., Martínez, J.L.F., 2021. Effects of climate variables on the COVID-19 outbreak in Spain. Int. J. Hyg Environ. Health 234, 113723.
Galvan, D., Effting, L., Cremasco, H., Adam Conte-Junior, C., 2020. Can socioeconomic, health, and safety data explain the spread of COVID-19 outbreak on Brazilian federative units? Int. J. Environ. Res. Publ. Health 17, 8921.
Galvan, D., Effting, L., Cremasco, H., Conte-Junior, C.A., 2021. The spread of the COVID-19 outbreak in Brazil: an overview by kohonen self-organizing map networks. Medicina 57, 235. https://doi.org/10.3390/medicina57030235.
Gamba-Sanchez, N., Rodriguez-Martinez, C., Sossa-Briceño, M., 2016. Epidemic activity of respiratory syncytial virus is related to temperature and rainfall in equatorial tropical countries. Epidemiol. Infect. 144, 2057–2063.
Garcia, J.S., da Silva, G.A., Arruda, M.A., Poppi, R.J., 2007. Application of Kohonen neural network to exploratory analyses of synchroton radiation x-ray fluorescence measurements of sunflower metalloproteins. X Ray Spectrom.: Int. J. 36, 122–129.
Gardner, E.G., Kelton, D., Poljak, Z., Van Kerkhove, M., von Dobschuetz, S., Greer, A.L., 2019. A case-crossover analysis of the impact of weather on primary cases of Middle East respiratory syndrome. BMC Infect. Dis. 19, 113. https://doi.org/10.1186/s12879-019-3729-5.
Gontijo, E.S.J., Herzsprung, P., Lechtenfeld, O.J., de Castro Bueno, C., Barth, A.C., Rosa, A.H., Friese, K., 2021. Multi-proxy approach involving ultrahigh resolution mass spectrometry and self-organising maps to investigate the origin and quality of sedimentary organic matter across a subtropical reservoir. Org. Geochem. 151, 104165. https://doi.org/10.1016/j.orggeochem.2020.104165.
Guarner, J., 2020. Three emerging coronaviruses in two Decades. Am. J. Clin. Pathol. 153, 420–421. https://doi.org/10.1093/ajcp/aqaa029.
Gupta, S., Raghuwanshi, G.S., Chanda, A., 2020. Effect of weather on COVID-19 spread in the US: a prediction model for India in 2020. Sci. Total Environ. 728, 138860. https://doi.org/10.1016/j.scitotenv.2020.138860.
Hammer, Ø., Harper, D.A., Ryan, P.D., 2001. PAST: paleontological statistics software package for education and data analysis. Palaeontol. Electron. 4, 9.
Hartono, P., 2020. Generating Similarity Map for COVID-19 Transmission Dynamics with Topological Autoencoder arXiv preprint arXiv:2004.01481.
He, Z., Chin, Y., Yu, S., Huang, J., Zhang, C.J., Zhu, K., Azarakhsh, N., Sheng, J., He, Y., Jayavanth, P., 2021. The influence of average temperature and relative humidity on new cases of COVID-19: time-series analysis. JMIR Public Health Surveillance 7, e20495.
Holdridge, L.R., Grenke, W.C., 1971. Forest Environments in Tropical Life Zones: a Pilot Study. Forest Environments in Tropical Life Zones: a Pilot Study.
Hopkins, Johns, 2021. Track Reported Cases of COVID-19 Coronavirus Resource Center. WWW Document, online).
Hridoy, A.-E.E., Mohiman, M.A., Tusher, S.M.S.H., Nowraj, S.Z.A., Rahman, M.A., 2021. Impact of meteorological parameters on COVID-19 transmission in Bangladesh: a spatiotemporal approach. Theor. Appl. Climatol. 144, 273–285.
Islam, A.R.M.T., Hasanuzzaman, M., Azad, M.A.K., Salam, R., Toshi, F.Z., Khan, M.S.I., Alam, G.M., Ibrahim, S.M., 2020. Effect of meteorological factors on COVID-19 cases in Bangladesh. Environ. Dev. Sustain. 1–24.
Islam, N., Shabnam, S., Erzurumluoglu, A.M., 2020. Meteorological factors and Covid-19 incidence in 310 regions across the world (preprint). Infectious Diseases (except HIV/AIDS). https://doi.org/10.1101/2020.03.27.20045658.
Islam, N., Bukhari, Q., Jameel, Y., Shabnam, S., Erzurumluoglu, A.M., Siddique, M.A., Massaro, J.M., D'Agostino, R.B., 2021. COVID-19 and climatic factors: a global analysis. Environ. Res. 193, 110355. https://doi.org/10.1016/j.envres.2020.110355.
Khan, W., Hussain, A., Khan, S.A., Al-Jumailey, M., Nawaz, R., Liatsis, P., 2021. Analysing the impact of global demographic characteristics over the COVID-19 spread using class rule mining and pattern matching, 8. Royal Society Open Science, p. 201823. https://doi.org/10.1098/rsos.201823.
Kohonen, T., 2001. Self-Organizing Maps, third ed. Springer Series in Information Sciences. Springer-Verlag, Berlin Heidelberg. https://doi.org/10.1007/978-3-642-56927-2.
Kowalski, C.H., da Silva, G.A., Godoy, H.T., Poppi, R.J., Augusto, F., 2013. Application of Kohonen neural network for evaluation of the contamination of Brazilian breast milk with polychlorinated biphenyls. Talanta 116, 315–321. https://doi.org/10.1016/j.talanta.2013.05.033.
Kubota, Y., Shiono, T., Kusumoto, B., Fujinuma, J., 2020. Multiple drivers of the COVID-19 spread: the roles of climate, international mobility, and region-specific conditions. PloS One 15, e0239385.
Kulkarni, H., Khandait, H., Narlawar, U.W., Rathod, P., Mamtani, M., 2021. Independent association of meteorological characteristics with initial spread of Covid-19 in India. Sci. Total Environ. 764, 142801. https://doi.org/10.1016/j.scitotenv.2020.142801.
Lawrence, M.G., 2005. The relationship between relative humidity and the dewpoint temperature in moist air: a simple conversion and applications. Bull. Am. Meteorol. Soc. 86, 225–234.
Leichtweis, B.G., de Faria Silva, L., da Silva, F.L., Peternelli, L.A., 2021. How the global health security index and environment factor influence the spread of COVID-19: a country level analysis. One Health 12, 100235. https://doi.org/10.1016/j.onehlt.2021.100235.
Lin, C., Lau, A.K.H., Fung, J.C.H., Guo, C., Chan, J.W.M., Yeung, D.W., Zhang, Y., Bo, Y., Hossain, M.S., Zeng, Y., Lao, X.Q., 2020. A mechanism-based parameterisation scheme to investigate the association between transmission rate of COVID-19 and meteorological factors on plains in China. Sci. Total Environ. 737, 140348. https://doi.org/10.1016/j.scitotenv.2020.140348.
Magurano, F., Baggieri, M., Marchi, A., Rezza, G., Nicoletti, L., Eleonora, B., Concetta, F., Stefano, F., Maedeh, K., Paola, B., Emilio, D., Silvia, G., 2021. SARS-CoV-2 infection: the environmental endurance of the virus can be influenced by the increase of temperature. Clin. Microbiol. Infect. 27, 289. https://doi.org/10.1016/j.cmi.2020.10.034 e5-289.e7.
Maier, B.F., Brockmann, D., 2020. Effective containment explains subexponential growth in recent confirmed COVID-19 cases in China. Science 368, 742–746.
Marcu, S., 2021. Towards sustainable mobility? The influence of the COVID-19 pandemic on Romanian mobile citizens in Spain. Sustainability 13, 4023.
Marquet, P., Geleyn, J.-F., 2015. Formulations of Moist Thermodynamics for Atmospheric Modelling arXiv preprint arXiv:1510.03239.
Melin, P., Monica, J.C., Sanchez, D., Castillo, O., 2020. Analysis of spatial spread relationships of coronavirus (COVID-19) pandemic in the world using self organizing maps. Chaos, Solit. Fractals 138, 109917. https://doi.org/10.1016/j.chaos.2020.109917.
Mollalo, A., Rivera, K.M., Vahedi, B., 2020. Artificial neural network modeling of novel coronavirus (COVID-19) incidence rates across the continental United States. Int. J. Environ. Res. Publ. Health 17, 4204.
Mouchtouri, V.A., Koureas, M., Kyritsi, M., Vontas, A., Kourentis, L., Sapounas, S., Rigakos, G., Petinaki, E., Tsiodras, S., Hadjichristodoulou, C., 2020. Environmental contamination of SARS-CoV-2 on surfaces, air-conditioner and ventilation systems. Int. J. Hyg Environ. Health 230, 113599.
Niazkar, H.R., Niazkar, M., 2020. Application of artificial neural networks to predict the COVID-19 outbreak. Glob. Health Research Pol. 5, 50. https://doi.org/10.1186/s41256-020-00175-y.
Notari, A., 2021. Temperature dependence of COVID-19 transmission. Sci. Total Environ. 763, 144390. https://doi.org/10.1016/j.scitotenv.2020.144390.
Nottmeyer, L.N., Sera, F., 2021. Influence of temperature, and of relative and absolute humidity on COVID-19 incidence in England - a multi-city time-series study. Environ. Res. 196, 110977. https://doi.org/10.1016/j.envres.2021.110977.
Oliveiros, B., Caramelo, L., Ferreira, N.C., Caramelo, F., 2020. Role of temperature and humidity in the modulation of the doubling time of COVID-19 cases (preprint). Public and Global Health. https://doi.org/10.1101/2020.03.05.20031872.
Pan, J., Yao, Y., Liu, Z., Meng, X., Ji, J.S., Qiu, Y., Wang, Weidong, Zhang, L., Wang, Weibing, Kan, H., 2021. Warmer weather unlikely to reduce the COVID-19 transmission: an ecological study in 202 locations in 8 countries. Sci. Total Environ. 753, 142272. https://doi.org/10.1016/j.scitotenv.2020.142272.
Pani, S.K., Lin, N.-H., RavindraBabu, S., 2020. Association of COVID-19 pandemic with meteorological parameters over Singapore. Sci. Total Environ. 740, 140112. https://doi.org/10.1016/j.scitotenv.2020.140112.
Paraskevis, D., Kostaki, E.G., Alygizakis, Nikiforos, Thomaidis, N.S., Cartalis, C., Tsiodras, S., Dimopoulos, M.A., 2021. A review of the impact of weather and climate variables to COVID-19: in the absence of public health measures high temperatures cannot probably mitigate outbreaks. Sci. Total Environ. 768, 144578. https://doi.org/10.1016/j.scitotenv.2020.144578.
Paynter, S., 2015. Humidity and respiratory virus transmission in tropical and temperate settings. Epidemiol. Infect. 143, 1110–1118. https://doi.org/10.1017/S0950268814002702.
Prata, D., Rodrigues, W., Bermejo, P.H.D.S., Moreira, M., Camargo, W., Lisboa, M., Reis, G.R., de Araujo, H.X., 2021. The relationship between (sub) tropical climates and the incidence of COVID-19. PeerJ 9, e10655.
Qi, H., Xiao, S., Shi, R., Ward, M.P., Chen, Y., Tu, W., Su, Q., Wang, W., Wang, X., Zhang, Z., 2020. COVID-19 transmission in Mainland China is associated with temperature and humidity: a time-series analysis. Sci. Total Environ. 728, 138778. https://doi.org/10.1016/j.scitotenv.2020.138778.
Raines, K.S., Doniach, S., Bhanot, G., 2020. The transmission of SARS-CoV-2 is likely comodulated by temperature and by relative humidity (preprint). Epidemiology. https://doi.org/10.1101/2020.05.23.20111278.
Ramírez, J.D., Florez, C., Muñoz, M., Hernández, C., Castillo, A., Gomez, S., Rico, A., Pardo, L., Barros, E.C., Castañeda, S., Ballesteros, N., Martínez, D., Vega, L., Jaimes, J.E., Cruz-Saavedra, L., Herrera, G., Patiño, L.H., Teherán, A.A., Gonzalez-Reiche, A.S., Hernandez, M.M., Sordillo, E.M., Simon, V., van Bakel, H., Paniz-Mondolfi, A., 2020. The arrival and spread of SARS-CoV-2 in Colombia. J. Med. Virol. 93, 1158–1163. https://doi.org/10.1002/jmv.26393.
Rodó, X., San-José, A., Kirchgatter, K., López, L., 2021. Changing climate and the COVID-19 pandemic: more than just heads or tails. Nat. Med. 27, 576–579. https://doi.org/10.1038/s41591-021-01303-y.

Rodriguez-Martinez, C., Sossa-Briceño, M., Acuña-Cordero, R., 2015. Relationship between meteorological conditions and respiratory syncytial virus in a tropical country. Epidemiol. Infect. 143, 2679–2686.
Rosario, D.K.A., Mutz, Y.S., Bernardes, P.C., Conte-Junior, C.A., 2020. Relationship between COVID-19 and weather: case study in a tropical country. Int. J. Hyg Environ. Health 229, 113587. https://doi.org/10.1016/j.ijheh.2020.113587.
Sajadi, M.M., Habibzadeh, P., Vintzileos, A., Shokouhi, S., Miralles-Wilhelm, F., Amoroso, A., 2020. Temperature, Humidity and Latitude Analysis to Predict Potential Spread and Seasonality for COVID-19 (SSRN Scholarly Paper No. ID 3550308). Social Science Research Network, Rochester, NY. https://doi.org/10.2139/ssrn.3550308.
Sanchez-Lorenzo, A., Vaquero-Martínez, J., Calbó, J., Wild, M., Santurtún, A., Lopez-Bustins, J.A., Vaquero, J.M., Folini, D., Antón, M., 2021. Did anomalous atmospheric circulation favor the spread of COVID-19 in Europe? Environ. Res. 194, 110626. https://doi.org/10.1016/j.envres.2020.110626.
Sartorius, B., Lawson, A., Pullan, R., 2021. Modelling and predicting the spatio-temporal spread of COVID-19, associated deaths and impact of key risk factors in England. Sci. Rep. 11, 1–11.
Seposo, X., Ng, C.F.S., Madaniyazi, L., 2021. Immediate and Delayed meteorological effects on COVID-19 time-varying infectiousness in tropical cities. Atmosphere 12, 513.
Shao, W., Xie, J., Zhu, Y., 2021. Mediation by human mobility of the association between temperature and COVID-19 transmission rate. Environ. Res. 194, 110608.
Spena, A., Palombi, L., Corcione, M., Carestia, M., Spena, V.A., 2020a. On the optimal indoor air conditions for SARS-CoV-2 inactivation. An enthalpy-based approach. Int. J. Environ. Res. Publ. Health 17, 6083.
Spena, A., Palombi, L., Corcione, M., Quintino, A., Carestia, M., Spena, V.A., 2020b. Predicting SARS-CoV-2 weather-induced seasonal virulence from atmospheric air enthalpy. Int. J. Environ. Res. Publ. Health 17, 9059.
Sulyok, M., Walker, M.D., 2021. Mobility and COVID-19 mortality across Scandinavia: a modeling study. Trav. Med. Infect. Dis. 41, 102039.
Sun, Z., Thilakavathy, K., Kumar, S.S., He, G., Liu, S.V., 2020. Potential factors influencing repeated SARS outbreaks in China. Int. J. Environ. Res. Publ. Health 17, 1633. https://doi.org/10.3390/ijerph17051633.
Tamerius, J.D., Shaman, J., Alonso, W.J., Bloom-Feshbach, K., Uejio, C.K., Comrie, A., Viboud, C., 2013. Environmental predictors of seasonal influenza epidemics across temperate and tropical climates. PLoS Pathog. 9, e1003194 https://doi.org/10.1371/journal.ppat.1003194.
Terfloth, L., Gasteiger, J., 2001. Neural networks and genetic algorithms in drug design. Drug Discov. Today 6, 102–108. https://doi.org/10.1016/S1359-6446(01)00173-8.
Tosepu, R., Gunawan, J., Effendy, D.S., Ahmad, L.O.A.I., Lestari, H., Bahar, H., Asfian, P., 2020. Correlation between weather and covid-19 pandemic in jakarta, Indonesia. Sci. Total Environ. 725, 138436. https://doi.org/10.1016/j.scitotenv.2020.138436.
Tushabe, F., 2020. Comparison of COVID-19 severity between tropical and non-tropical countries. Int. J. Infect. 7 https://doi.org/10.5812/iji.104142.
Vesanto, J., 1999. SOM-based data visualization methods. Intell. Data Anal. 3, 111–126.
Vollmer, M.A., Mishra, S., Unwin, H.J.T., Gandy, A., Mellan, T.A., Bradley, V., Zhu, H., Coupland, H., Hawryluk, I., Hutchinson, M., 2020. Report 20: Using Mobility to Estimate the Transmission Intensity of COVID-19 in Italy: a Subnational Analysis with Future Scenarios. medRxiv.
Wang, J., Tang, K., Feng, K., Lin, X., Lv, W., Chen, K., Wang, F., 2021. Impact of temperature and relative humidity on the transmission of COVID-19: a modelling study in China and the United States. BMJ open 11, e043863. https://doi.org/10.1136/bmjopen-2020-043863.
Wei, J.-T., Liu, Y.-X., Zhu, Y.-C., Qian, J., Ye, R.-Z., Li, C.-Y., Ji, X.-K., Li, H.-K., Qi, C., Wang, Y., 2020. Impacts of transportation and meteorological factors on the transmission of COVID-19. Int. J. Hyg Environ. Health 230, 113610.
Wheeler, S.M., 2015. Built landscapes of metropolitan regions: an international typology. J. Am. Plann. Assoc. 81, 167–190. https://doi.org/10.1080/01944363.2015.1081567.
WHO, 2020a. COVID 19 Public Health Emergency of International Concern (PHEIC). Global research and innovation forum: towards a research roadmap.
WHO, 2020b. WHO announces COVID-19 outbreak a pandemic [WWW Document]. URL https://www.euro.who.int/en/health-topics/health-emergencies/coronavirus-covid-19/news/news/2020/3/who-announces-covid-19-outbreak-a-pandemic (accessed 12.14.20).
Wu, Y., Jing, W., Liu, J., Ma, Q., Yuan, J., Wang, Y., Du, M., Liu, M., 2020. Effects of temperature and humidity on the daily new cases and new deaths of COVID-19 in 166 countries. Sci. Total Environ. 729, 139051. https://doi.org/10.1016/j.scitotenv.2020.139051.
Xie, J., Zhu, Y., 2020. Association between ambient temperature and COVID-19 infection in 122 cities from China. Sci. Total Environ. 724, 138201. https://doi.org/10.1016/j.scitotenv.2020.138201.
Yahya, B.M., Yahya, F.S., Thannoun, R.G., 2021. COVID-19 prediction analysis using artificial intelligence procedures and GIS spatial analyst: a case study for Iraq. Appl. Geomat. 13, 481–491. https://doi.org/10.1007/s12518-021-00365-4.
Yang, X.-D., Li, H.-L., Cao, Y.-E., 2021. Influence of meteorological factors on the COVID-19 transmission with season and geographic location. Int. J. Environ. Res. Publ. Health 18, 484.
Zhou, P., Yang, X.-L., Wang, X.-G., Hu, B., Zhang, L., Zhang, W., Si, H.-R., Zhu, Y., Li, B., Huang, C.-L., Chen, H.-D., Chen, J., Luo, Y., Guo, H., Jiang, R.-D., Liu, M.-Q., Chen, Y., Shen, X.-R., Wang, X., Zheng, X.-S., Zhao, K., Chen, Q.-J., Deng, F., Liu, L.-L., Yan, B., Zhan, F.-X., Wang, Y.-Y., Xiao, G.-F., Shi, Z.-L., 2020. A pneumonia outbreak associated with a new coronavirus of probable bat origin. Nature 579, 270–273. https://doi.org/10.1038/s41586-020-2012-7.
Zhou, Y., Xu, R., Hu, D., Yue, Y., Li, Q., Xia, J., 2020. Effects of human mobility restrictions on the spread of COVID-19 in Shenzhen, China: a modelling study using mobile phone data. Lancet Dig. Health 2, e417–e424.